# *PARP1* Gene Variation and Microglial Activity on [$^{11}$C]PBR28 PET in Older Adults at Risk for Alzheimer's Disease

Sungeun Kim[1-3,6], Kwangsik Nho[1,2,6], Shannon L. Risacher[1,3], Mark Inlow[4], Shanker Swaminathan[1], Karmen K. Yoder[1,3,6], Li Shen[1-3,6], John D. West[1], Brenna C. McDonald[1,3,5,6], Eileen F. Tallman[1,3], Gary D. Hutchins[1,3,6], James W. Fletcher[1,6], Martin R. Farlow[3,5], Bernardino Ghetti[3,7], and Andrew J. Saykin[1-3,5,6,8,*]

[1] Center for Neuroimaging, Department of Radiology and Imaging Sciences
[2] Center for Computational Biology and Bioinformatics
[3] Indiana Alzheimer Disease Center, Indiana University School of Medicine, Indianapolis, IN, USA
[4] Department of Mathematics, Rose-Hulman Institute of Technology, Terre Haute, IN, USA
[5] Department of Neurology
[6] Indiana Institute for Biomedical Imaging Sciences
[7] Department of Pathology and Laboratory Medicine
[8] Department of Medical and Molecular Genetics, Indiana University School of Medicine, Indianapolis, IN, USA

**Abstract.** Increasing evidence suggests that inflammation is one pathophysiological mechanism in Alzheimer's disease (AD). Recent studies have identified an association between the poly (ADP-ribose) polymerase 1 (*PARP1*) gene and AD. This gene encodes a protein that is involved in many biological functions, including DNA repair and chromatin remodeling, and is a mediator of inflammation. Therefore, we performed a targeted genetic association analysis to investigate the relationship between the *PARP1* polymorphisms and brain microglial activity as indexed by [$^{11}$C]PBR28 positron emission tomography (PET). Participants were 26 non-Hispanic Caucasians in the Indiana Memory and Aging Study (IMAS). PET data were intensity-normalized by injected dose/total body weight. Average [$^{11}$C]PBR28 standardized uptake values (SUV) from 6 bilateral regions of interest (thalamus, frontal, parietal, temporal, and cingulate cortices, and whole brain gray matter) were used as endophenotypes. Single nucleotide polymorphisms (SNPs) with 20% minor allele frequency that were within +/- 20 kb of the *PARP1* gene were included in the analyses. Gene-level association analyses were performed using a dominant genetic model with translocator protein (18-kDa) (*TSPO*) genotype, age at PET scan, and gender as covariates. Analyses were performed with and without *APOE* ε4 status as a covariate. Associations with [$^{11}$C]PBR28 SUVs from thalamus and cingulate were significant at corrected $p<0.014$ and $<0.065$, respectively. Subsequent multi-marker analysis with cingulate [$^{11}$C]PBR28 SUV showed that

* Corresponding author.

L. Shen et al. (Eds.): MBIA 2013, LNCS 8159, pp. 150–158, 2013.

individuals with the "C" allele at rs6677172 and "A" allele at rs61835377 had higher [$^{11}$C]PBR28 SUV than individuals without these alleles (corrected $P$<0.03), and individuals with the "G" allele at rs6677172 and "G" allele at rs61835377 displayed the opposite trend (corrected $P$<0.065). A previous study with the same cohort showed an inverse relationship between [$^{11}$C]PBR28 SUV and brain atrophy at a follow-up visit, suggesting possible protective effect of microglial activity against cortical atrophy. Interestingly, all 6 AD and 2 of 3 LMCI participants in the current analysis had one or more copies of the "GG" allele combination, associated with lower cingulate [$^{11}$C]PBR28 SUV, suggesting that this gene variant warrants further investigation.

# 1 Introduction

Alzheimer's disease (AD) is the most common form of dementia and a progressive, degenerative disorder resulting in loss of memory at first, and eventually affecting all cognition and behavior. Increasing evidence suggests that failed or dysregulated immune response is one candidate mechanism contributing to the pathogenesis of AD [1-4]. Recent large-scale genome-wide association studies (GWAS) have identified several candidate genetic variants in *CLU, CR1, ABCA7, BIN1, PICALM, CD33, CD2AP, EPHA1* and *MS4A6A/MS4A6E* in addition to the most robust candidate gene, *APOE* [5-8]. Several of these genes are known to be involved in immune system functioning [2, 3].

The poly (ADP-ribose) polymerase 1 (*PARP1*) gene plays roles in many biological functions including chromatin remodeling, DNA repair, telomere maintenance, and is known to be a mediator of inflammation via regulation of NF-kB and other transcription factors [9]. Several studies have investigated the *PARP1* gene in relation to AD [9-12], reporting risk and protective haplotypes [10], enhanced activity of *PARP1* in AD brain [12], and association with rate of hippocampal atrophy [11].

The peripheral benzodiazepine receptor (PBR; official name – translocator protein (18kDa), *TSPO*) is expressed at low levels in relatively inactive microglia. Microglia play an early critical role in activation of the immune response in the central nervous system [13]. Because activated microglia apparently express higher levels of TSPO than inactive microglia, PBR has been considered a useful marker to detect neuroinflammation. Positron emission tomography (PET) imaging with the radioligand [$^{11}$C]N-acetyl-N-(2-methoxybenzyl)-2-phenoxy-5-pyridinamine ([$^{11}$C]PBR28) has shown high selectivity for the TSPO in vivo [14]. The goal of this study was to investigate the relationship between *PARP1* gene variation and microglial activity indexed by [$^{11}$C]PBR28 PET.

# 2 Materials and Methods

## 2.1 Participants

In order to reduce the potential bias of population stratification, analyses were restricted to 26 non-Hispanic Caucasian participants from the Indiana Memory and Aging Study (IMAS) cohort. IMAS is an ongoing longitudinal study, including

euthymic older adults with subjective cognitive decline (SCD), defined by memory concerns (e.g., self-perceived decline) in the context of cognitive test performance that is within the normal range, patients with early and late amnestic mild cognitive impairment (EMCI and LMCI) or mild AD, and age-matched cognitively normal controls (NC) without significant cognitive complaints or concerns. Details regarding participant selection criteria and characterization have been described previously [15, 16]. This study was approved by the Indiana University School of Medicine Institutional Review Board and written informed consent was obtained from all participants. The 26 participants in the study included 7 NC, 6 CC, 4 EMCI, 3 LMCI, and 6 AD. Table 1 shows the sample characteristics. *APOE* ε2/ε3/ε4 genotype, genome-wide genotyping data, and [$^{11}$C]PBR28 PET scans were available for all participants. It has been shown that the rs6971 variant in the *TSPO* gene affects in vivo binding affinity of the [$^{11}$C]PBR28 ligand [17, 18]. Subjects with genotypes corresponding to mixed or high affinity sites at the TSPO were included in the study; one "non-binder" (low-affinity TSPO phenotype) was excluded.

**Table 1.** Sample Characteristics

| Characteristics | All | NC | SCD | EMCI | LMCI | AD |
|---|---|---|---|---|---|---|
| Number of Samples | 26 | 7 | 6 | 4 | 3 | 6 |
| Age at PET scan (years; mean±SD) | 71.3±7.49 | 68.4±2.64 | 70.3±9.81 | 74.5±6.95 | 72.7±5.69 | 72.7±10.48 |
| Education (years; mean±SD) | 16.4±2.78 | 16.3±1.70 | 17.3±1.21 | 15.5±4.12 | 15.3±3.06 | 16.5±4.18 |
| Gender (M/F) | 9/17 | 1/6 | 2/4 | 2/2 | 2/1 | 2/4 |
| *APOE* (ε4-/ε4+) | 15/11 | 3/4 | 4/2 | 3/1 | 2/1 | 3/3 |
| *TSPO* genotype (Mixed/High) | 9/17 | 2/5 | 1/5 | 3/1 | 2/1 | 1/5 |

## 2.2 Data and Quality Control Procedure

**Genetic Data.** Genotyping was performed on genomic DNA from blood using the Illumina HumanOmniExpress BeadChip (Illumina, Inc., San Diego, CA), which contains over 700,000 SNP (single nucleotide polymorphism) markers, according to the manufacturer's protocols (Infinium HD Assay; Super Protocol Guide; Rev. A, May 2008). *APOE* ε2/ε3/ε4 genotyping was separately performed. All genotype data, including two *APOE* SNPs (rs429358 and rs7412), underwent standard quality control (QC) assessment using PLINK v1.07 [19] as described previously [20]. SNPs were

imputed using the 1000 Genomes reference panel (http://www.1000genomes.org/) following the Enhancing Neuroimaging Genetics through Meta-Analysis 2 (ENIGMA 2) imputation protocol (http://enigma.loni.ucla.edu/wp-content/uploads/2012/07/ENIGMA2_1KGP_v3.pdf [27 July 2012]). Some imputed SNPs were removed based on the following criteria: $r^2 < 0.5$ between imputed and the nearest genotyped SNPs. After all QC steps, 96 SNPs with 20% minor allele frequency that were within +/- 20 kb of the *PARP1* gene were included in the analyses.

**Imaging Data.** Dynamic PET scans, acquired on a Siemens HR+, were initiated with injection of 512.33±75.83 MBq of [$^{11}$C]PBR28. Data were acquired for 90 min (10x30s, 9x60s, 2x180s, 8x300s, 3x600s). PET data were processed as described previously [18]. In brief, PET data were motion-corrected and normalized to MNI space. Static images were created from data between 40-90 min, and were normalized by injected dose/total body weight to produce standardized uptake value (SUV) images. Regions of interest (ROIs) were generated from each subject's anatomic MRI, which was concurrently acquired on a Siemens Tim Trio using an MPRAGE sequence and post processed using Freesurfer v4.0.1 (http://surfer.nmr.mgh.harvard.edu/). Average [$^{11}$C]PBR28 SUV values were extracted from 6 bilateral ROIs (thalamus, frontal, parietal, temporal, and cingulate cortices, and whole brain gray matter including cingulate and sensory motor areas) and were used as endophenotypes.

### 2.3 Statistical Analyses

In order to investigate the overall influence of *PARP1* variants on microglial activity (as indexed by average [$^{11}$C]PBR28 SUV in 6 bilateral ROIs), a set-based analysis method in PLINK was adopted. In brief, this method evaluates the association of individual SNPs in a given set with a given phenotype and selects a set of independent (based on $r^2$ threshold) and significant (based on p threshold) SNPs to represent the overall effect of the set. Then, the significance of the overall set effect is assessed using permutation to correct for multiple SNPs within a set while taking into account the linkage disequilibrium (LD) structure among SNPs. In this study, the analysis was performed using the following settings: (1) $r^2$ threshold: 0.3, (2) p threshold: 0.05, (3) maximum number of independent and significant SNPs: 99999 in order to use all independent and significant SNPs, and (4) number of permutation: 50,000. Due to the limited number of samples, only a dominant genetic model was assessed. Age at PET scan, gender and TSPO genotype based on the rs6971 SNP were added to the model as covariates. Analysis was performed with and without *APOE* ε4 status as a covariate.

When more than one independent and significant SNP were identified from significant associations, a subsequent multi-marker analysis was performed using a haplotype analysis method in PLINK with the same set of covariates in the model. The association p-value was corrected for multiple testing (the number of SNP combinations) using 50,000 permutations. Although the PLINK set-based approach provides the significance of the *PARP1* gene and the list of independent and significant SNPs in *PARP1*, it does not show the joint influence of multiple SNPs on average

[$^{11}$C]PBR28 SUV values. This multi-marker method allowed us to further study the combinatorial effect of multiple SNPs on average [$^{11}$C]PBR28 SUV values.

## 3 Results

*PARP1* variation was associated with average [$^{11}$C]PBR28 SUV from thalamus at $p<0.014$ after adjusting for *APOE* ε4 status. This association was driven by rs874583, located in the intergenic area downstream of the gene. Samples with one or more minor allele ("C") of rs874583 showed higher SUV in thalamus (Fig.1). Another association with average [$^{11}$C]PBR28 SUV in cingulate showed marginal significance at $p<0.065$ after *APOE* ε4 adjustment and was driven by two SNPs (rs6677172 and rs61835377). Both SNPs are intergenic and downstream of the gene. Minor alleles of these two SNPs (rs6677172: "G", rs61835377: "A") showed an inverse relationship with average [$^{11}$C]PBR28 SUV in cingulate.

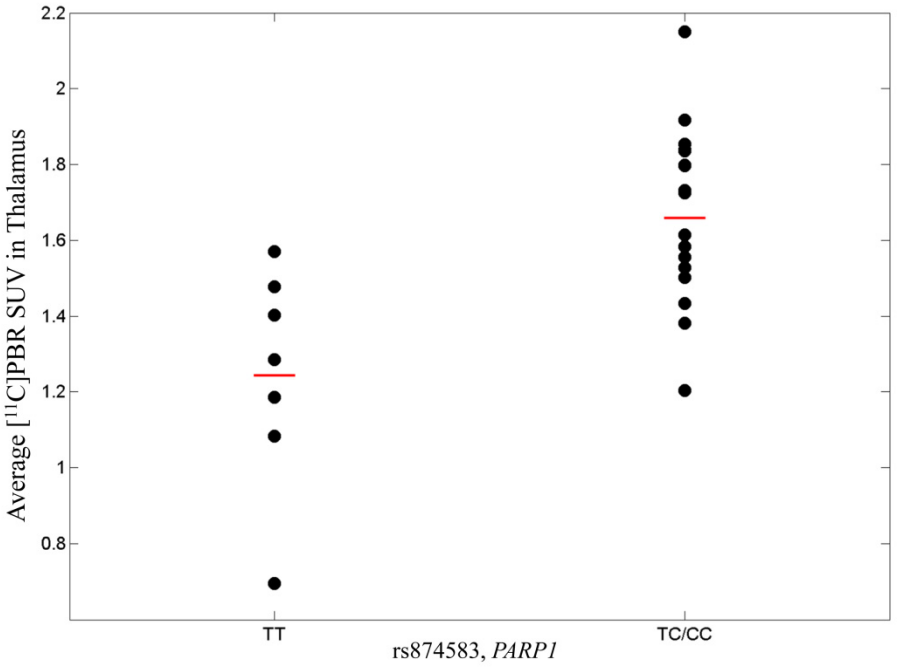


**Fig. 1.** Average [$^{11}$C]PBR28 SUV in thalamus in *PARP1* variant, rs874583 (minor allele: C). SUV was adjusted for age at PET scan, gender, TSPO genotype, and *APOE* ε4 status. The horizontal bars represent the mean PBR SUV for each genotype group.

Two SNPs (rs6677172 and rs61835377) were jointly associated with average [$^{11}$C]PBR28 SUV in cingulate. Therefore, a subsequent multi-marker analysis was performed to investigate influence of the allele combination of the SNPs on the same phenotype. The analysis identified three different combinations of alleles

("CA","CG", and "GG"), of which two were significantly associated with average [$^{11}$C]PBR28 SUV in cingulate at uncorrected p<0.05. One ("CA") was significant after correction for multiple testing at corrected p<0.05. Table 2 summarizes the multi-marker analysis results. "CA" allele combination was positively correlated with the [$^{11}$C]PBR28 SUV and "GG" allele combination was negatively correlated with the phenotype. Average [$^{11}$C]PBR28 SUVs in cingulate are displayed in Fig.2 for samples with and without "CA" allele combination (Fig.2 (a)) and with and without "GG" allele combination (Fig.2 (b)). Interestingly, all 6 AD and 2 out of 3 LMCI participants in the current analysis had one or two copies of the "GG" allele combination, associated with lower average cingulate [$^{11}$C]PBR28 SUV.

**Table 2.** Multi-marker analysis results. Allele, F, BETA, P, and Corrected P represent allele combination, frequency of allele combination, regression coefficient, uncorrected p, and corrected p for the number of allele combination, respectively.

| PHENOTYPE | Allele | F | BETA | P | Corrected P |
|---|---|---|---|---|---|
| Average [$^{11}$C]PBR28 SUV Cingulate | CA | 0.212 | 0.204 | 0.0105 | 0.02962 |
| | GG | 0.385 | -0.164 | 0.0241 | 0.06426 |

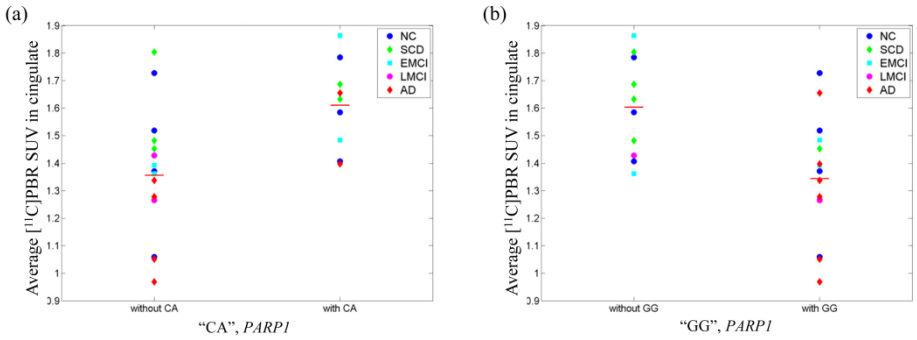


**Fig. 2.** Scatter plots of average [$^{11}$C]PBR28 SUV in cingulate for (a) "CA" allele group and (b) "GG" allele group. Average PBR SUV was adjusted for age at PET scan, gender, *TSPO* genotype, and *APOE* ε4 status. The horizontal bars represent the mean PBR SUV for each allele group.

## 4 Conclusions

This preliminary study investigated the relationship between variation in *PARP1* and microglial activity indexed by [$^{11}$C]PBR28 PET and identified significant associations of the gene with average [$^{11}$C]PBR28 SUVs in thalamus and cingulate. The subsequent multi-marker analysis also identified two allele combinations from the gene-based analysis associated with average [$^{11}$C]PBR28 SUV in cingulate. These identified associations suggested the role of *PARP1* in immune activation. Microglia can perform different functions [1, 13] and the specific role of microglial activation in the

current sample of older adults at risk for AD is not known and may include both adaptive and adverse aspects. However, one interesting observation in the current study is that 8 out of 9 participants with AD or LMCI had one or two copies of the "GG" allele combination, which was associated with lower average [$^{11}$C]PBR28 SUV in cingulate compared to non-"GG" carriers. A previous study with the same cohort showed an inverse relationship between [$^{11}$C]PBR28 SUV and brain atrophy at a follow-up visit, suggesting a possible protective effect of microglial activity against cortical atrophy [21], which warrants further investigation. A major limitation of this preliminary study is the modest sample size which attenuates power, and the findings require replication in larger, independent samples as a future direction. The relationship between *PARP1* and microglial activity also warrants experimental molecular validation. Despite the limited sample size, this preliminary study identified interesting significant in vivo associations in an important pathway related to AD pathobiology. This approach combining neuroimaging and genetics data appears promising and can be applied to many related fields of research.

**Acknowledgment.** This study was supported in part by the National Institutes of Health, National Institute on Aging (R01 AG19771, P30AG10133), National Library of Medicine (R01 LM011360), National Science Foundation (IIS-1117335), NIH Clinical and Translational Sciences Institute Pre-doctoral Training Fellowship (Training Grant TL1 RR025759), and National Library of Medicine (K99 LM011384).

## References

1. Hickman, S.E., Allison, E.K., El Khoury, J.: Microglial dysfunction and defective beta-amyloid clearance pathways in aging Alzheimer's disease mice. J. Neurosci. 28, 8354–8360 (2008)
2. Jones, L., Holmans, P.A., Hamshere, M.L., Harold, D., Moskvina, V., Ivanov, D., Pocklington, A., Abraham, R., Hollingworth, P., Sims, R., Gerrish, A., et al.: Genetic evidence implicates the immune system and cholesterol metabolism in the aetiology of Alzheimer's disease. PLoS One 5, e13950 (2010)
3. Lambert, J.C., Grenier-Boley, B., Chouraki, V., Heath, S., Zelenika, D., Fievet, N., Hannequin, D., Pasquier, F., Hanon, O., Brice, A., Epelbaum, J., Berr, C., Dartigues, J.F., Tzourio, C., Campion, D., Lathrop, M., Amouyel, P.: Implication of the immune system in Alzheimer's disease: evidence from genome-wide pathway analysis. J. Alzheimers Dis. 20, 1107–1118 (2010)
4. Zhang, R., Miller, R.G., Madison, C., Jin, X., Honrada, R., Harris, W., Katz, J., Forshew, D.A., McGrath, M.S.: Systemic immune system alterations in early stages of Alzheimer's disease. J. Neuroimmunol. 256, 38–42 (2013)
5. Harold, D., Abraham, R., Hollingworth, P., Sims, R., Gerrish, A., Hamshere, M.L., Pahwa, J.S., Moskvina, V., Dowzell, K., Williams, A., Jones, N., Thomas, C., et al.: Genome-wide association study identifies variants at CLU and PICALM associated with Alzheimer's disease. Nat. Genet. 41, 1088–1093 (2009)
6. Hollingworth, P., Harold, D., Sims, R., Gerrish, A., Lambert, J.C., Carrasquillo, M.M., Abraham, R., Hamshere, M.L., Pahwa, J.S., Moskvina, V., et al.: Common variants at ABCA7, MS4A6A/MS4A4E, EPHA1, CD33 and CD2AP are associated with Alzheimer's disease. Nat. Genet. 43, 429–435 (2011)

7. Lambert, J.C., Heath, S., Even, G., Campion, D., Sleegers, K., Hiltunen, M., Combarros, O., Zelenika, D., Bullido, M.J., Tavernier, B., Letenneur, L., Bettens, K., et al.: Genome-wide association study identifies variants at CLU and CR1 associated with Alzheimer's disease. Nat. Genet. 41, 1094–1099 (2009)
8. Naj, A.C., Jun, G., Beecham, G.W., Wang, L.S., Vardarajan, B.N., Buros, J., Gallins, P.J., Buxbaum, J.D., Jarvik, G.P., Crane, P.K., Larson, E.B., Bird, T.D., et al.: Common variants at MS4A4/MS4A6E, CD2AP, CD33 and EPHA1 are associated with late-onset Alzheimer's disease. Nat. Genet. 43, 436–441 (2011)
9. Kauppinen, T.M., Suh, S.W., Higashi, Y., Berman, A.E., Escartin, C., Won, S.J., Wang, C., Cho, S.H., Gan, L., Swanson, R.A.: Poly(ADP-ribose)polymerase-1 modulates microglial responses to amyloid beta. J. Neuroinflammation 8, 152 (2011)
10. Liu, H.P., Lin, W.Y., Wu, B.T., Liu, S.H., Wang, W.F., Tsai, C.H., Lee, C.C., Tsai, F.J.: Evaluation of the poly(ADP-ribose) polymerase-1 gene variants in Alzheimer's disease. J. Clin. Lab. Anal. 24, 182–186 (2010)
11. Nho, K., Corneveaux, J.J., Kim, S., Lin, H., Risacher, S.L., Shen, L., Swaminathan, S., Ramanan, V.K., Liu, Y., Foroud, T., Inlow, M.H., Siniard, A.L., et al.: Whole-exome sequencing and imaging genetics identify functional variants for rate of change in hippocampal volume in mild cognitive impairment. Mol. Psychiatry (2013), doi:10.1038/mp.2013.24
12. Strosznajder, J.B., Czapski, G.A., Adamczyk, A., Strosznajder, R.P.: Poly(ADP-ribose) polymerase-1 in amyloid beta toxicity and Alzheimer's disease. Mol. Neurobiol. 46, 78–84 (2012)
13. Gehrmann, J., Matsumoto, Y., Kreutzberg, G.W.: Microglia: intrinsic immuneffector cell of the brain. Brain Res. Brain Res. Rev. 20, 269–287 (1995)
14. Kreisl, W.C., Fujita, M., Fujimura, Y., Kimura, N., Jenko, K.J., Kannan, P., Hong, J., Morse, C.L., Zoghbi, S.S., Gladding, R.L., Jacobson, S., Oh, U., Pike, V.W., Innis, R.B.: Comparison of [(11)C]-(R)-PK 11195 and [(11)C]PBR28, two radioligands for translocator protein (18 kDa) in human and monkey: Implications for positron emission tomographic imaging of this inflammation biomarker. Neuroimage 49, 2924–2932 (2010)
15. Risacher, S.L., Wudunn, D., Pepin, S.M., MaGee, T.R., McDonald, B.C., Flashman, L.A., Wishart, H.A., Pixley, H.S., Rabin, L.A., Pare, N., Englert, J.J., Schwartz, E., Curtain, J.R., West, J.D., O'Neill, D.P., Santulli, R.B., Newman, R.W., Saykin, A.J.: Visual contrast sensitivity in Alzheimer's disease, mild cognitive impairment, and older adults with cognitive complaints. Neurobiol. Aging 34, 1133–1144 (2013)
16. Saykin, A.J., Wishart, H.A., Rabin, L.A., Santulli, R.B., Flashman, L.A., West, J.D., McHugh, T.L., Mamourian, A.C.: Older adults with cognitive complaints show brain atrophy similar to that of amnestic MCI. Neurology 67, 834–842 (2006)
17. Owen, D.R., Yeo, A.J., Gunn, R.N., Song, K., Wadsworth, G., Lewis, A., Rhodes, C., Pulford, D.J., Bennacef, I., Parker, C.A., St Jean, P.L., Cardon, L.R., Mooser, V.E., Matthews, P.M., Rabiner, E.A., Rubio, J.P.: An 18-kDa translocator protein (TSPO) polymorphism explains differences in binding affinity of the PET radioligand PBR28. J. Cereb. Blood Flow. Metab. 32, 1–5 (2012)
18. Yoder, K.K., Nho, K., Risacher, S.L., Kim, S., Shen, L., Saykin, A.J.: Influence of TSPO genotype on [11C]PBR28 standardized uptake values. Journal of Nuclear Medicine (2013), doi:10.2967/jnumed.112.118885
19. Purcell, S., Neale, B., Todd-Brown, K., Thomas, L., Ferreira, M.A., Bender, D., Maller, J., Sklar, P., de Bakker, P.I., Daly, M.J., Sham, P.C.: PLINK: a tool set for whole-genome association and population-based linkage analyses. Am. J. Hum. Genet. 81, 559–575 (2007)

20. Shen, L., Kim, S., Risacher, S.L., Nho, K., Swaminathan, S., West, J.D., Foroud, T., Pankratz, N., Moore, J.H., Sloan, C.D., Huentelman, M.J., Craig, D.W., Dechairo, B.M., Potkin, S.G., Jack Jr., C.R., Weiner, M.W., Saykin, A.J.: Whole genome association study of brain-wide imaging phenotypes for identifying quantitative trait loci in MCI and AD: A study of the ADNI cohort. Neuroimage 53, 1051–1063 (2010)
21. Risacher, S.L., Kim, S., Yoder, K.K., Shen, L., West, J.D., McDonald, B.C., Wang, Y., Nho, K., Tallman, E., Hutchins, G.D., Fletcher, J.W., Ghetti, B., Gao, S., Farlow, M.R., Saykin, A.J.: Relationship of microglial activation measured by [11C]PBR28 PET, atrophy on MRI, and plasma biomarkers in individuals with and at-risk for Alzheimer's disease. In: Alzheimer's Association International Conference 2013 (Abstract number: 39417) (2013)